doi:10.1093/brain/aws137 Brain 2012: 135; 2350–2357 | 2350

BRAIN
A JOURNAL OF NEUROLOGY

Structural substrates for resting network disruption in temporal lobe epilepsy

Natalie L. Voets,[1,2] Christian F. Beckmann,[2,3,4] David M. Cole,[3] SeokJun Hong,[1] Andrea Bernasconi[1] and Neda Bernasconi[1]

1 Neuroimaging of Epilepsy Laboratory, Department of Neurology and McConnell Brain Imaging Centre, Montreal Neurological Institute and Hospital, McGill University, Montreal, Quebec H3A 2B4 Canada
2 University of Oxford FMRIB Centre, Oxford OX3 9DU, UK
3 Centre for Neuroscience, Division of Experimental Medicine, Imperial College London, London SW7 2AZ, UK
4 MIRA Institute for Biomedical Technology and Technical Medicine, University of Twente, 7500 AW Enschede, The Netherlands

Correspondence to: Neda Bernasconi, MD PhD,
Montreal Neurological Institute (WB-322),
3801 University Street,
Montreal, Quebec,
H3A 2B4 Canada
E-mail: neda@bic.mni.mcgill.ca

Magnetic resonance imaging methods that measure interregional brain signalling at rest have been advanced as powerful tools to probe organizational properties of functional networks. In drug-resistant temporal lobe epilepsy, resting functional magnetic resonance imaging studies have primarily employed region of interest approaches that preclude a comprehensive evaluation of large-scale functional interactions. In line with the distributed nature of structural damage in this condition, we set out to quantify connectivity across the entire range of resting networks. Furthermore, we assessed whether connectivity is driven by co-localized structural pathology. We obtained resting state, diffusion tensor and anatomical imaging data in 35 patients with temporal lobe epilepsy and 20 healthy subjects on a 3 T scanner. Resting state networks were identified using independent component analysis, which allows an objective whole-brain quantification of functional connectivity. We performed group comparisons before and after correcting for voxel-wise grey matter density. In addition, we identified voxel-wise associations between resting connectivity and white matter coherence indexed by fractional anisotropy. Compared with controls, patients showed altered (typically reduced) functional connectivity between the hippocampus, anterior temporal, precentral cortices and the default mode and sensorimotor networks. Reduced network integration of the hippocampus was explained by variations in grey matter density, while functional connectivity of the parahippocampus, and frontal and temporal neocortices showed atypical associations with white matter coherence within pathways carrying connections of these regions. Our multimodal imaging study suggests that in temporal lobe epilepsy, cortical atrophy and microstructural white matter damage impact functional resting connectivity.

Keywords: functional MRI; diffusion tensor; networks; epilepsy
Abbreviation: TLE = temporal lobe epilepsy

Introduction

Temporal lobe epilepsy (TLE) is the most frequent form of drug-resistant focal epilepsy. Although mesiotemporal sclerosis is the hallmark of this condition, structural changes affecting the neocortex of the fronto-central, temporal and parietal regions (Bernhardt *et al*., 2009, 2010) as well as the axonal fibre bundles that link them (Focke *et al*., 2008; Concha *et al*., 2009), suggest

Received November 21, 2011. Revised March 19, 2012. Accepted April 18, 2012. Advance Access publication June 4, 2012

widespread abnormalities of brain organization. Indeed, using graph theoretical analysis to quantify topological and organizational properties of complex systems, we recently showed evidence for altered large-scale structural networks (Bernhardt *et al*., 2011).

MRI methods that measure interregional brain signalling have been advanced as powerful tools to probe organizational properties of functional networks (Biswal *et al*., 1995; McKeown *et al*., 1998; Beckmann *et al*., 2005). In particular, studies correlating signal fluctuations while healthy volunteers rest in the scanner have revealed a highly robust set of resting state networks (Greicius *et al*., 2003; Beckmann *et al*., 2005) that are believed to reflect synchronous firing of discrete neuronal populations (Fox and Raichle, 2007). In TLE, resting functional MRI studies have mainly focused on quantifying signalling between regions known to be involved in seizure activity, particularly among medial temporal lobe structures (Bettus *et al*., 2009, 2010; Pereira *et al*., 2010), and those that form the 'default mode' state (Frings *et al*., 2009; Liao *et al*., 2010, 2011; Zhang *et al*., 2010). The majority of these studies used region of interest analytical approaches that preclude a comprehensive evaluation of large-scale functional interactions (Cole *et al*., 2010).

Notable correspondence between resting functional and structural networks has been shown in healthy subjects (Honey *et al*., 2007, 2009; Vincent *et al*., 2007; Skudlarski *et al*., 2008). Abnormal (typically reduced) resting signalling from the hippocampus in patients with Alzheimer's disease and schizophrenia (Wang *et al*., 2006; Zhou *et al*., 2008), in whom hippocampal atrophy is prevalent (Apostolova *et al*., 2006; Velakoulis *et al*., 2006), raises the possibility that abnormal mesiotemporal functional connectivity in TLE may at least partly reflect structural pathology, rather than epileptogenic or functionally compensatory processes to which it has been attributed (Bettus *et al*., 2009, 2010; Morgan *et al*., 2010). The potential effect of structural damage on resting signal coupling, however, remains largely unknown.

Our aim was to determine the extent to which resting connectivity in patients with drug-resistant TLE is associated with co-localized structural pathology. In line with the distributed nature of structural damage in this condition, we used independent component analysis that optimizes sensitivity to wide-scale resting signalling, correcting for voxel-wise grey matter density. In addition, we assessed the relationship between resting signalling and white matter microstructure using tract-based spatial statistics.

Materials and methods

Participants

We studied 35 consecutive right-handed patients with drug-resistant TLE being evaluated for epilepsy surgery at the Montreal Neurological Institute (MNI; 16 males, mean age = 34.3 ± 8.9 years, range = 19–53). The diagnosis and lateralization of the seizure focus into left TLE ($n = 19$) and right TLE ($n = 16$) were determined by a comprehensive evaluation including detailed history, video-EEG telemetry and neuroimaging in all. None of the patients had a mass lesion (tumour, vascular malformation or malformations of cortical development) or traumatic brain injury. Twenty patients underwent surgery. We determined surgical outcome according to the Engel classification scheme (Engel, 1993) at a mean follow-up time of 18 ± 5.6 months. Fourteen patients had an outcome Class I (seven Class Ia, six Class Ib, one Class Id), three Class II, two Class III and one of Class IV. Following qualitative histopathological analysis, hippocampal sclerosis was detected in all 15 patients in whom specimens were available. In the remaining five, hippocampal specimens were unsuitable for histopathology due to subpial aspiration.

The control group consisted of 20 healthy volunteers (11 males, mean age = 29.2 ± 6.7 years, range = 20–48 years). As controls were slightly younger than patients (left TLE, $t = -2.231$, $P = 0.03$; right TLE, $t = -1.757$, $P = 0.09$), age was used as a nuisance variable in all analyses. Demographic and clinical data are presented in Table 1.

The Ethics Committee of the Montreal Neurological Institute and Hospital approved this study and written informed consent was obtained from all participants in accordance with the standards of the Declaration of Helsinki.

Magnetic resonance imaging acquisition

Magnetic resonance images were acquired on a 3 T Siemens Trio Trim scanner using a 32-channel phased-array head coil. Resting blood oxygen level-dependent data were acquired in each subject using an echo-planar imaging sequence (repetition time = 2020 ms, echo time = 30 ms, flip angle = 90°, field of view = 256 × 256 mm^2, slice thickness = 4 mm, 34 slices with no gap, voxel size 4 × 4 × 4 mm^3, 5 min acquisition and 220 volumes). Participants were instructed to lie still with their eyes closed while remaining awake. To minimize signal loss and distortion affecting orbitofrontal and mesiotemporal regions, slices were angled at an oblique coronal orientation. The diffusion tensor imaging protocol consisted of a twice-refocused echo-planar imaging sequence (63 axial slices, voxel resolution 2 × 2 × 2 mm^3, repetition time = 8.4 s, echo time = 90 ms, diffusion-sensitized images in 64 diffusion directions

Table 1 Demographic and clinical data

Group	Males	Age (years)	Onset	Duration	FC	Surgery	Engel-I
Controls ($n = 20$)	11	29.2 ± 6.7 (20–48)	–	–	–	–	–
Left TLE ($n = 19$)	7	34.4 ± 8.0 (19–45)	20.3 ± 10.3 (4–44)	14.6 ± 10 (1–35)	3	8	5
Right TLE ($n = 16$)	8	34.1 ± 10.2 (20–53)	21.3 ± 13.6 (2–48)	11.6 ± 10.4 (1–35)	4	12	9

Age, age at seizure onset and duration of epilepsy are presented in mean ± SD (range) years. FC = febrile convulsions.

with $b = 1000\,s/mm^2$ along with one non-diffusion weighted volume). T_1-weighted images were acquired using a 3D MP-RAGE, providing isotropic voxels of $1 \times 1 \times 1\,mm^3$.

Resting state functional magnetic resonance imaging analysis

The analysis was conducted using tools from the FMRIB Software library (www.fmrib.ox.ac.uk/fsl). The preprocessing consisted of the removal of the first 12 s from each time series to ensure magnetization equilibrium, brain extraction, motion correction, high-pass filtering with a frequency cut-off at 100 s, spatial smoothing at 5 mm full-width half-maximum, intensity normalization and affine linear registration to the MNI 152 standard template. Absolute head motion was below 1.5 mm for all 55 subjects. Subsequently, resting data were analysed in three parts: first, we identified resting state networks common to our 20 healthy controls using independent component analysis implemented in MELODIC (Beckmann *et al*., 2005). For this analysis, the resting scans for all controls were combined into a single 4D data set, which was then decomposed into spatio-temporal components that represent large-scale patterns of co-activating voxels accounting for statistically independent sources of variation in the measured functional MRI signal (Beckmann *et al*., 2005). Automatic model-order estimation identified 44 independent spatial components. Of these, we selected 10 components for further analysis based on visual neuroanatomical correspondence and cross-correlation ($P < 0.05$) with consistently identified resting state networks described in the literature (Beckmann *et al*., 2005) (Supplementary Fig. 1). On the basis of the regions involved (Supplementary Table 1), putative roles have been proposed for each of these networks in executive control/language (Network 3), fronto-parietal perception (Network 2), sensorimotor functions (Networks 4 and 5), 'default mode' physiology/attention (Networks 1, 6 and 7), audition (Network 8) and vision (Networks 9 and 10). Next, we obtained for every subject (i.e. controls and patients) the spatial map corresponding to each of these group-level networks using a two-step dual regression approach (Khalili-Mahani *et al*., 2012). As spatial maps have their own characteristic time-course, the first regression identified temporal correspondence between each subject's data and each group-level component. The second regression then identified voxels in each subject's data that shared this time-course, thus producing individual-level spatial maps corresponding to each group-level component. The resulting subject-specific spatial components were normalized for changes in amplitude of the resting signal fluctuations to ensure that resulting signal differences could be explained only by variations in the shape of the time-course (i.e. are attributable to changes in the strength of signal correlations). This procedure generates subject-specific maps (one per original component) of resting functional connectivity; maps can then be compared between groups.

Statistical tests for group differences in functional connectivity ($P < 0.05$, cluster corrected) were conducted within a general linear model framework using the FMRIB Software Library's randomize (v2.1) using 5000 permutations. We chose this approach, rather than constraining analyses to a given network, to improve sensitivity to changes occurring outside the boundaries defining each component's spatial map. Based on our group size of 55 ($df = 52$), we set the cluster-forming threshold to $t = 2$ ($P < 0.05$). To constrain analyses to the cortex, we constructed a group mean mask by averaging the grey matter segmentations obtained from each subject's T_1-weighted MRI.

Grey matter density confound analysis

To remove potential variations in resting functional MRI signal fluctuations related to grey matter volume, we repeated the resting group comparison using voxel-wise grey matter density as a covariate in the linear model.

Diffusion tract-based spatial statistics analysis

Functional connectivity abnormalities that remained unchanged after correcting for grey matter density were used as covariates of interest in voxel-wise analyses of white matter fractional anisotropy. To minimize potential interactions between grey matter density and white matter microstructure, potentially obscuring the interpretation of resting connectivity, this analysis was performed on the original, non-grey matter corrected clusters.

Following motion/eddy current correction, a diffusion tensor model was fitted at every voxel to derive fractional anisotropy maps, which were non-linearly registered to group-specific templates created from controls and patients. The resulting fractional anisotropy images were temporally concatenated into a single 4D file and averaged to create a mean 'skeleton', representing the centre of all white matter tracts for each group-pair (controls and left TLE/controls and right TLE) onto which subject-specific fractional anisotropy values were projected. Finally, using tract-based spatial statistics, we performed group comparisons through a 2D implementation of randomize permutation testing described above to identify associations between voxel-wise fractional anisotropy and resting connectivity values derived from each cluster showing group differences not accounted for by grey matter volume. In diffusion tensor imaging tractography approaches, white matter tracts are segmented by estimating the directional information of water diffusion of coherently oriented axons. However, fibre bundles may cross, split or merge within individual voxels, affecting fractional anisotropy measurements. To aid interpretation of findings in regions of crossing fibres, TBSS X software (Jbabdi *et al*., 2010) was used *post hoc* to visualize directional information of two different fibre populations modelled at the level of single voxels.

Results

Resting state connectivity: relation to grey matter density

Compared with healthy controls, patients with left TLE showed reduced functional connectivity between ipsilateral temporal (lateral and temporopolar) cortices and anterior default mode network (Network 7, $P = 0.024$; Fig. 1A), which persisted after correction for grey matter density. Patients with right TLE showed reduced functional connectivity relative to controls between the ipsilateral parahippocampal region and the medial default mode network (Network 1, $P = 0.043$; Fig. 1B), between the right hippocampus and left lateral temporal cortex and the posterior default mode network (Network 6, $P = 0.009$; Fig. 1C) and between the ipsilateral frontal (premotor and supplementary motor) cortices and the extended sensorimotor network (Network 4, $P = 0.012$; Fig. 1D). While removing the variability associated

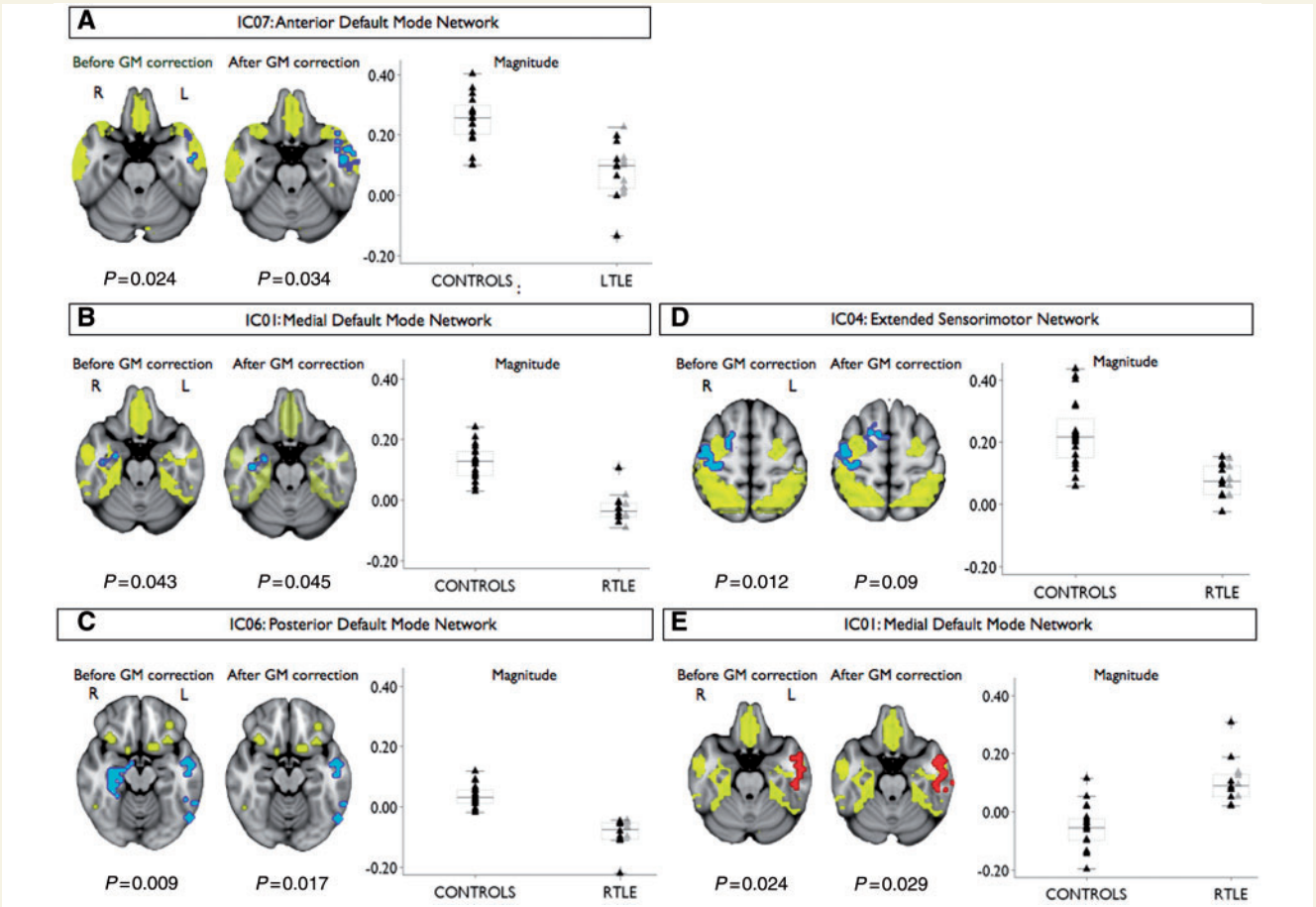

Figure 1 Whole-brain group-wise results of permutation tests (cluster-corrected to $P < 0.05$) conducted within each of the 10 resting state networks in patients with left (LTLE, **A**) and right TLE (RTLE, **B–E**). T_1-weighted axial sections are overlaid with the resting state network (transparent yellow) and clusters showing significantly reduced (blue) or increased (red) functional connectivity to this network. Plots of the connectivity effect magnitude extracted from each cluster are shown (patients with and without hippocampal atrophy are represented by grey and black triangles, respectively). IC = independent component; GM = grey matter; L = left; R = right.

with grey matter density abolished decreased signalling between the right hippocampus and posterior default mode network, the decreased functional connectivity between this network and the left lateral temporal cortex remained unchanged (Fig. 1C). On the other hand, decreases in functional connectivity between the medial default mode network and the parahippocampal region (Fig. 1B), and between the extended sensorimotor network and the frontal cortices (Fig. 1D) persisted after grey matter correction. Finally, in patients with right TLE, the medial default mode network (Network 1) showed increased functional connectivity with the left temporal pole ($P = 0.024$; Fig. 1E), which also persisted after grey matter correction.

Since permutation tests identify any region where the relationship between the functional MRI signal and the main time-course of a network differs between groups, it is possible that portions of clusters fall outside the boundary of a given network (Fig. 1A and D). We repeated the resting connectivity analyses using the spatial maps for each component to constrain statistical comparisons within network boundaries. This network-specific analysis identified the same clusters found through the whole-brain analysis. Understandably, changes were located within networks, as this approach cannot detect anomalies that fall outside network boundaries. Furthermore, as fewer multiple-comparison corrections are needed to compare with whole-brain analysis, the network-specific approach showed increased sensitivity to within-network group differences in the sensorimotor network in patients with left TLE and in the left fronto-parietal network in patients with right TLE (Supplementary Fig. 2).

Relationship between altered functional connectivity and fibre pathway coherence

In left TLE (Fig. 2), the decrease in resting connectivity seen between the left temporal cortices and the anterior default mode network (Network 7) was positively associated with fractional anisotropy in the ipsilateral temporal lobe white matter ($P = 0.02$). Specifically, reduced resting signalling between this region and anterior default mode network in patients correlated

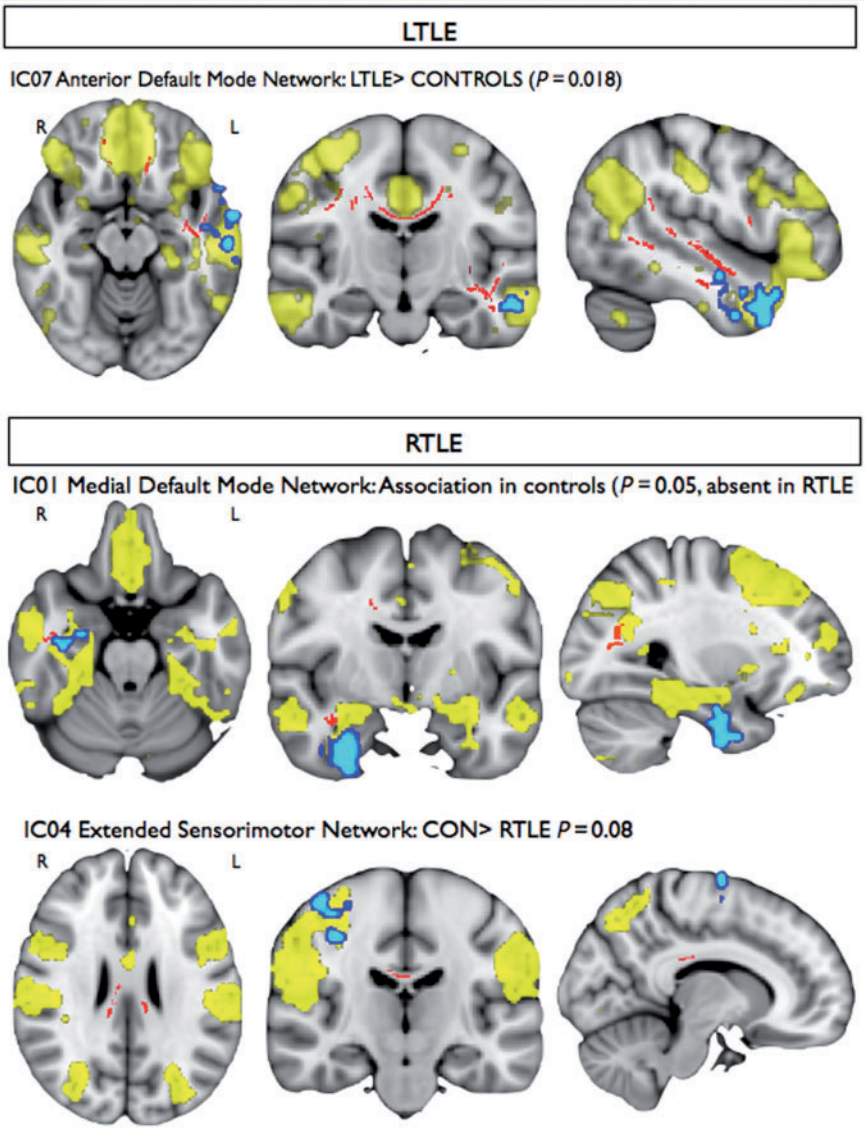

Figure 2 Group-wise difference in association between resting functional connectivity and structural fibre coherence. Whole-brain tract-based spatial statistics results depict voxels (red) showing correlations between fractional anisotropy and resting functional connectivity (blue) to specific resting state networks (yellow) for clusters showing altered resting connectivity that were not explained by grey matter density. Results indicate strong associations between resting connectivity abnormalities and fractional anisotropy. Directional information for two fibres is presented in Supplementary Figs 3 and 4 to aid anatomical interpretation. CON = controls; IC = independent component; LTLE = left TLE; RTLE = right TLE.

with reduced fractional anisotropy along the ipsilateral uncinate and thalamic radiation, the inferior and superior longitudinal fasciculi and the corpus callosum ($P = 0.022$). These associations were not seen in controls, resulting in a significant group difference (left TLE > controls, $P = 0.018$).

In patients with right TLE (Fig. 2), two of the three resting connectivity findings that were not explained by variations in cortical volume also showed altered associations with white matter coherence compared with controls. While in the latter, functional connectivity between the right parahippocampal gyrus and the medial default mode network (Network 1) was positively associated with fractional anisotropy along the right inferior longitudinal fasciculus and the callosum ($P = 0.05$), this association was not present in patients with right TLE. Similarly, there was a trend for a stronger correlation in controls than in patients with right TLE between functional connectivity in the right precentral gyrus to the sensorimotor network and fractional anisotropy along the callosum ($P = 0.08$). No association was found between fractional anisotropy and increased resting connectivity found between the left temporopolar cortex and the medial default mode network.

Group comparisons of structure–function associations between right TLE and controls co-localized to regions with strong confidence of a single fibre orientation. On the other hand, the left TLE temporal lobe cluster localized to a region with a high probability of crossing fibres (Supplementary Figs 3 and 4).

Discussion

Resting functional MRI studies in TLE have typically shown reduced connectivity involving ipsilateral mesiotemporal structures (Bettus *et al*., 2009, 2010; Morgan *et al*., 2010; Pereira *et al*., 2010) and altered integration with widespread regions of the default mode network (Frings *et al*., 2009; Zhang *et al*., 2010, 2011). Given the overlap of these signalling abnormalities with regions implicated electrographically in seizure generation and spread (Chabardes *et al*., 2005), it is tempting to interpret these findings as indicative of the epileptogenic network. However, previous studies in TLE analysed functional connectivity in predefined regions of interest or single networks, and did not take cortical and white matter damage into account. We opted for an objective whole-brain quantification of resting connectivity through independent component analysis, a technique that decomposes the signal into spatiotemporal components. The benefit of this approach is flexibility in data modelling to identify potentially wide-ranging abnormalities without *a priori* hypotheses (Cole *et al*., 2010). This is of particular importance since in TLE pathological interactions involve distributed brain regions (Bernhardt *et al*., 2011). In addition, abnormal functional connectivity may extend beyond a given network and involve multiple regions, such as the recruitment of the right frontal lobe into the left-lateralized language network (Waites *et al*., 2006). Specifically, our voxel-wise dual regression approach quantifies the degree to which individual voxels contribute to each resting-state network and compares groups through permutation testing. Thus, clusters may be identified within or outside a given resting network, without bias to either. Moreover, this approach is less affected by subtle variability in the specific regions that cluster into a network across studies, or even during a single resting functional MRI experiment, known as the non-stationarity problem (Cole *et al*., 2010). For example, the hippocampus is identified in the default mode networks in some but not all studies (Greicius *et al*., 2004). Finally, the simultaneous analysis of all networks increases sensitivity in cases where individual voxels contribute to multiple networks. On the other hand, the network selection is based on visual inspection of independent spatial components. We have addressed this limitation by performing a cross-correlation with template resting state networks (Beckmann *et al*., 2005) and selecting only the 10 that were strongly correlated with the Beckmann *et al.* (2005) set.

We found resting anomalies in patients with left TLE restricted to the ipsilateral temporal lobe, whereas in right TLE, we observed additional changes in the ipsilateral sensorimotor cortices and contralateral temporal lobe. These regions overlap notably with neural systems supporting memory, language and motor functions. Behavioural explanations for resting findings can only be speculative at the moment, as definitive studies relating resting functional MRI, task functional MRI and neuropsychological performance in the same patients remain lacking. Impaired tactile discrimination has been reported in patients with TLE [see Grant (2005) for review] and may account for our findings of reduced functional integration of precentral regions in the sensorimotor network. Activity within and correlation between midline posterior cingulate and hippocampal structures that form core parts of the default mode network can be specifically manipulated through episodic memory tasks (Vincent *et al*., 2006) on which patients with TLE are often impaired (Bell *et al*., 2011). The spatial correspondence between brain regions forming these neurocognitive systems and those showing altered resting functional connectivity, therefore, offer the tentative hypothesis that reduced functional connectivity in these networks may reflect patient-specific behavioural organization.

Observed differences in the extent of resting connectivity abnormalities between left and right TLE's are in agreement with a previous resting default mode network connectivity study using independent component analysis (Zhang *et al*., 2010), but are in contrast with others describing bilateral temporal changes in left TLE (Bettus *et al*., 2009; Pereira *et al*., 2010). Aside from possible differences related to patient selection criteria, divergences may also stem from the analytical approach (region of interest-based versus whole-brain), making a direct comparison between studies difficult. Nevertheless, our observation of greater functional disconnectivity in right TLE supports the possibility of hemisphere-specific vulnerability to injury potentially related to asymmetric brain development (Sun and Walsh, 2006). In this scenario, abnormalities would occur during a time window of left hemisphere susceptibility when right hemisphere homologues, due to a more advanced stage of development, are relatively spared. Asymmetric resting functional connectivity differences notably parallel our previous structural observations in a separate group of patients with TLE. When assessing morphometric markers of brain development, we found bilaterally increased sulco-gyral complexity in right TLE, whereas such changes were unilateral in left TLE (Voets *et al*., 2011).

In TLE, the most parsimonious explanation for widespread structural abnormalities is that, at the scale of neuroimaging, this condition is represented by an altered configuration of grey matter regions and their interconnecting white matter tracts, which is somehow reflected in abnormal functional connectivity. Our multimodal MRI study indeed revealed that structural variations influence resting connectivity in TLE. Notably, reduced functional connectivity between the epileptic hippocampus and the posterior default mode network in our patients with right TLE was explained by variability in grey matter volume, suggesting altered signal coupling may be an indirect marker of hippocampal damage. Outside of the mesiotemporal lobe, while grey matter variations seemed not to alter resting connectivity, complex interactions were found with white matter microstructure. However, we cannot confidently disentangle grey from white matter contributions, as fractional anisotropy may co-vary with grey matter volume (Douaud *et al*., 2007). While there was a direct relation between reduced functional connectivity and fractional anisotropy in left TLE, in right TLE associations normally seen in controls were lost. These findings parallel dichotomies in cortical thickness correlations we reported previously (Bernhardt *et al*., 2008). Reduced coherence of white matter bundles secondary to axonal degeneration could explain the loss of normally present structural–functional associations. On the other hand, abnormal myelination (Thom *et al*., 2000) or maturation (Thom *et al*., 2001) may alter

the efficiency of functional communication, resulting in a pathological association not seen in controls.

In left TLE, the decrease in resting connectivity seen between the left temporal neocortex and the default mode network was positively associated with fractional anisotropy in the ipsilateral temporal lobe white matter. On the other hand, in our patients with right TLE, the left temporal neocortex showed both reduced and increased functional connectivity with default mode network findings that were not accounted for by our structural measures and possibly indicate co-existing pathological processes. Notably, our previous morphometric analyses in right TLE showed extensive thinning (Bernhardt *et al*., 2010), as well as bilaterally increased gyral complexity (Voets *et al*., 2011) in this region. While atrophy may be associated with decreased functional communication, it is conceivable that increased cortical complexity is reflective of aberrant, potentially increased fibre connectivity, which could in turn enhance functional interactions.

Importantly, even though it is commonly assumed that functional connectivity reflects structural connectivity, the exact relationship between structure and function might not be straightforward (Damoiseaux and Greicius, 2009). While diffusion tensor imaging supports dependence between resting functional and structural connectivity in specific regions in both the healthy and diseased brain (van den Heuvel *et al*., 2008; Greicius *et al*., 2009; Mars *et al*., 2011), functional connectivity has also been observed in regions where there is little or no structural connectivity (Lowe *et al*., 2008; Uddin *et al*., 2008). This probably indicates signal correlations mediated by indirect structural connections (i.e. via a third region) or polysynaptic pathways that do not have a structural correlate (Honey *et al*., 2009; Lu *et al*., 2011). Finally, intensity abnormalities in the temporo-polar region may blur the grey–white matter transition (Ryvlin *et al*., 2002; Sankar *et al*., 2008), making it difficult to segment confidently tissue compartments and obscuring the interpretation of the underlying pathophysiological substrate.

Overall our results suggest that morphology impacts function in TLE, although a contribution of the epileptic activity cannot be entirely excluded. Structural damage may explain previously reported discrepancy between increased interictal EEG synchronicity and decreased mesiotemporal functional MRI signalling (Bettus *et al*., 2009).

Acknowledgements

The authors would like to express gratitude to the patients who participated in this study, and are grateful to N. Filippini and G. Douaud for helpful discussions.

Funding

This work was supported by the Canadian Institutes of Health Research (CIHR MOP-93815, CIHR MOP-57840). Personal support for N.L.V. was provided by the Canadian Centres of Excellence in Commercialization and Research and the UK Medical Research Council.

Supplementary material

Supplementary material is available at *Brain* online.

References

Apostolova LG, Dutton RA, Dinov ID, Hayashi KM, Toga AW, Cummings JL, et al. Conversion of mild cognitive impairment to Alzheimer disease predicted by hippocampal atrophy maps. Arch Neurol 2006; 63: 693–9.

Beckmann CF, DeLuca M, Devlin JT, Smith SM. Investigations into resting-state connectivity using independent component analysis. Philos Trans R Soc Lond B Biol Sci 2005; 360: 1001–13.

Bell B, Lin JJ, Seidenberg M, Hermann B. The neurobiology of cognitive disorders in temporal lobe epilepsy. Nat Rev Neurol 2011; 7: 154–64.

Bernhardt BC, Bernasconi N, Concha L, Bernasconi A. Cortical thickness analysis in temporal lobe epilepsy: reproducibility and relation to outcome. Neurology 2010; 74: 1776–84.

Bernhardt BC, Chen Z, He Y, Evans AC, Bernasconi N. Graph-theoretical analysis reveals disrupted small-world organization of cortical thickness correlation networks in temporal lobe epilepsy. Cereb Cortex 2011; 21: 2147–57.

Bernhardt BC, Worsley KJ, Besson P, Concha L, Lerch JP, Evans AC, et al. Mapping limbic network organization in temporal lobe epilepsy using morphometric correlations: insights on the relation between mesiotemporal connectivity and cortical atrophy. Neuroimage 2008; 42: 515–24.

Bernhardt BC, Worsley KJ, Kim H, Evans AC, Bernasconi A, Bernasconi N. Longitudinal and cross-sectional analysis of atrophy in pharmacoresistant temporal lobe epilepsy. Neurology 2009; 72: 1747–54.

Bettus G, Bartolomei F, Confort-Gouny S, Guedj E, Chauvel P, Cozzone PJ, et al. Role of resting state functional connectivity MRI in presurgical investigation of mesial temporal lobe epilepsy. J Neurol Neurosurg Psychiatry 2010; 81: 1147–54.

Bettus G, Guedj E, Joyeux F, Confort-Gouny S, Soulier E, Laguitton V, et al. Decreased basal fMRI functional connectivity in epileptogenic networks and contralateral compensatory mechanisms. Hum Brain Mapp 2009; 30: 1580–91.

Biswal B, Yetkin FZ, Haughton VM, Hyde JS. Functional connectivity in the motor cortex of resting human brain using echo-planar MRI. Magn Reson Med 1995; 34: 537–41.

Chabardes S, Kahane P, Minotti L, Tassi L, Grand S, Hoffmann D, et al. The temporopolar cortex plays a pivotal role in temporal lobe seizures. Brain 2005; 128(Pt 8): 1818–31.

Cole DM, Smith SM, Beckmann CF. Advances and pitfalls in the analysis and interpretation of resting-state FMRI data. Front Syst Neurosci 2010; 4: 8.

Concha L, Beaulieu C, Collins DL, Gross DW. White-matter diffusion abnormalities in temporal-lobe epilepsy with and without mesial temporal sclerosis. J Neurol Neurosurg Psychiatry 2009; 80: 312–9.

Damoiseaux JS, Greicius MD. Greater than the sum of its parts: a review of studies combining structural connectivity and resting-state functional connectivity. Brain Struct Funct 2009; 213: 525–33.

Douaud G, Smith S, Jenkinson M, Behrens T, Johansen-Berg H, Vickers J, et al. Anatomically related grey and white matter abnormalities in adolescent-onset schizophrenia. Brain 2007; 130(Pt 9): 2375–86.

Engel J Jr. Update on surgical treatment of the epilepsies. Summary of the Second International Palm Desert Conference on the Surgical Treatment of the Epilepsies (1992). Neurology 1993; 43: 1612–7.

Focke NK, Yogarajah M, Bonelli SB, Bartlett PA, Symms MR, Duncan JS. Voxel-based diffusion tensor imaging in patients with mesial temporal lobe epilepsy and hippocampal sclerosis. Neuroimage 2008; 40: 728–37.

Fox MD, Raichle ME. Spontaneous fluctuations in brain activity observed with functional magnetic resonance imaging. Nat Rev Neurosci 2007; 8: 700–11.

Frings L, Schulze-Bonhage A, Spreer J, Wagner K. Remote effects of hippocampal damage on default network connectivity in the human brain. J Neurol 2009; 256: 2021–9.
Grant AC. Interictal perceptual function in epilepsy. Epilepsy Behav 2005; 6: 511–9.
Greicius MD, Krasnow B, Reiss AL, Menon V. Functional connectivity in the resting brain: a network analysis of the default mode hypothesis. Proc Natl Acad Sci USA 2003; 100: 253–8.
Greicius MD, Srivastava G, Reiss AL, Menon V. Default-mode network activity distinguishes Alzheimer's disease from healthy aging: evidence from functional MRI. Proc Natl Acad Sci USA 2004; 101: 4637–42.
Greicius MD, Supekar K, Menon V, Dougherty RF. Resting-state functional connectivity reflects structural connectivity in the default mode network. Cereb Cortex 2009; 19: 72–8.
Honey CJ, Kotter R, Breakspear M, Sporns O. Network structure of cerebral cortex shapes functional connectivity on multiple time scales. Proc Natl Acad Sci USA 2007; 104: 10240–5.
Honey CJ, Sporns O, Cammoun L, Gigandet X, Thiran JP, Meuli R, et al. Predicting human resting-state functional connectivity from structural connectivity. Proc Natl Acad Sci USA 2009; 106: 2035–40.
Jbabdi S, Behrens TE, Smith SM. Crossing fibres in tract-based spatial statistics. Neuroimage 2010; 49: 249–56.
Khalili-Mahani N, Zoethout RM, Beckmann CF, Baerends E, de Kam ML, Soeter RP, et al. Effects of morphine and alcohol on functional brain connectivity during "resting state": a placebo-controlled crossover study in healthy young men. Hum Brain Mapp 2012; 33: 1003–18.
Liao W, Zhang Z, Pan Z, Mantini D, Ding J, Duan X, et al. Altered functional connectivity and small-world in mesial temporal lobe epilepsy. PLoS One 2010; 5: e8525.
Liao W, Zhang Z, Pan Z, Mantini D, Ding J, Duan X, et al. Default mode network abnormalities in mesial temporal lobe epilepsy: a study combining fMRI and DTI. Hum Brain Mapp 2011; 32: 883–95.
Lowe MJ, Beall EB, Sakaie KE, Koenig KA, Stone L, Marrie RA, et al. Resting state sensorimotor functional connectivity in multiple sclerosis inversely correlates with transcallosal motor pathway transverse diffusivity. Hum Brain Mapp 2008; 29: 818–27.
Lu J, Liu H, Zhang M, Wang D, Cao Y, Ma Q, et al. Focal pontine lesions provide evidence that intrinsic functional connectivity reflects polysynaptic anatomical pathways. J Neurosci 2011; 31: 15065–71.
Mars RB, Jbabdi S, Sallet J, O'Reilly JX, Croxson PL, Olivier E, et al. Diffusion-weighted imaging tractography-based parcellation of the human parietal cortex and comparison with human and macaque resting-state functional connectivity. J Neurosci 2011; 31: 4087–100.
McKeown MJ, Makeig S, Brown GG, Jung TP, Kindermann SS, Bell AJ, et al. Analysis of fMRI data by blind separation into independent spatial components. Hum Brain Mapp 1998; 6: 160–88.
Morgan VL, Gore JC, Abou-Khalil B. Functional epileptic network in left mesial temporal lobe epilepsy detected using resting fMRI. Epilepsy Res 2010; 88: 168–78.
Pereira FR, Alessio A, Sercheli MS, Pedro T, Bilevicius E, Rondina JM, et al. Asymmetrical hippocampal connectivity in mesial temporal lobe epilepsy: evidence from resting state fMRI. BMC Neurosci 2010; 11: 66.
Pereira FR, Alessio A, Sercheli MS, Pedro T, Bilevicius E, Rondina JM, et al. Asymmetrical hippocampal connectivity in mesial temporal lobe epilepsy: evidence from resting state fMRI. BMC Neurosci 2010; 11: 66.
Ryvlin P, Coste S, Hermier M, Mauguiere F. Temporal pole MRI abnormalities in temporal lobe epilepsy. Epileptic Disord 2002; 4 (Suppl 1): S33–9.
Sankar T, Bernasconi N, Kim H, Bernasconi A. Temporal lobe epilepsy: differential pattern of damage in temporopolar cortex and white matter. Hum Brain Mapp 2008; 29: 931–44.
Skudlarski P, Jagannathan K, Calhoun VD, Hampson M, Skudlarska BA, Pearlson G. Measuring brain connectivity: diffusion tensor imaging validates resting state temporal correlations. Neuroimage 2008; 43: 554–61.
Sun T, Walsh CA. Molecular approaches to brain asymmetry and handedness. Nat Rev Neurosci 2006; 7: 655–62.
Thom M, Holton JL, D'Arrigo C, Griffin B, Beckett A, Sisodiya S, et al. Microdysgenesis with abnormal cortical myelinated fibres in temporal lobe epilepsy: a histopathological study with calbindin D-28-K immunohistochemistry. Neuropathol Appl Neurobiol 2000; 26: 251–7.
Thom M, Sisodiya S, Harkness W, Scaravilli F. Microdysgenesis in temporal lobe epilepsy: a quantitative and immunohistochemical study of white matter neurones. Brain 2001; 124(Pt 11): 2299–309.
Uddin LQ, Mooshagian E, Zaidel E, Scheres A, Margulies DS, Kelly AM, et al. Residual functional connectivity in the split-brain revealed with resting-state functional MRI. Neuroreport 2008; 19: 703–9.
van den Heuvel M, Mandl R, Luigjes J, Hulshoff Pol H. Microstructural organization of the cingulum tract and the level of default mode functional connectivity. J Neurosci 2008; 28: 10844–51.
Velakoulis D, Wood SJ, Wong MT, McGorry PD, Yung A, Phillips L, et al. Hippocampal and amygdala volumes according to psychosis stage and diagnosis: a magnetic resonance imaging study of chronic schizophrenia, first-episode psychosis, and ultra-high-risk individuals. Arch Gen Psychiatry 2006; 63: 139–49.
Vincent JL, Patel GH, Fox MD, Snyder AZ, Baker JT, Van Essen DC, et al. Intrinsic functional architecture in the anaesthetized monkey brain. Nature 2007; 447: 83–6.
Vincent JL, Snyder AZ, Fox MD, Shannon BJ, Andrews JR, Raichle ME, et al. Coherent spontaneous activity identifies a hippocampal-parietal memory network. J Neurophysiol 2006; 96: 3517–31.
Voets NL, Bernhardt BC, Kim H, Yoon U, Bernasconi N. Increased temporolimbic cortical folding complexity in temporal lobe epilepsy. Neurology 2011; 76: 138–44.
Waites AB, Briellmann RS, Saling MM, Abbott DF, Jackson GD. Functional connectivity networks are disrupted in left temporal lobe epilepsy. Ann Neurol 2006; 59: 335–43.
Wang L, Zang Y, He Y, Liang M, Zhang X, Tian L, et al. Changes in hippocampal connectivity in the early stages of Alzheimer's disease: evidence from resting state fMRI. Neuroimage 2006; 31: 496–504.
Zhang X, Tokoglu F, Negishi M, Arora J, Winstanley S, Spencer DD, et al. Social network theory applied to resting-state fMRI connectivity data in the identification of epilepsy networks with iterative feature selection. J Neurosci Methods 2011; 199: 129–39.
Zhang Z, Lu G, Zhong Y, Tan Q, Liao W, Wang Z, et al. Altered spontaneous neuronal activity of the default-mode network in mesial temporal lobe epilepsy. Brain Res 2010; 1323: 152–60.
Zhou Y, Shu N, Liu Y, Song M, Hao Y, Liu H, et al. Altered resting-state functional connectivity and anatomical connectivity of hippocampus in schizophrenia. Schizophr Res 2008; 100: 120–32.